PCCP

ROYAL SOCIETY OF CHEMISTRY

PAPER

View Article Online
View Journal | View Issue

Cite this: *Phys. Chem. Chem. Phys.*, 2020, **22**, 4823

Potential molecular semiconductor devices: cyclo-C_n (n = 10 and 14) with higher stabilities and aromaticities than acknowledged cyclo-C_{18}†

Mengyang Li,[a] Zhibin Gao,[b] Yanbo Han,[a] Yaoxiao Zhao,[a] Kun Yuan,[c] Shigeru Nagase,[d] Masahiro Ehara[e] and Xiang Zhao*[a]

Received 11th January 2020,
Accepted 7th February 2020

DOI: 10.1039/d0cp00167h

rsc.li/pccp

The successful synthesis and isolation of cyclo-C_{18} in experiments is a ground-breaking development in carbon rings. Herein, we studied the thermodynamic stabilities of cyclo-C_n ($4 \leq n \leq 34$) with hybrid density functional theory. When $n = 4N + 2$ (N is an integer), cyclo-C_n were thermodynamically stable. In particular, cyclo-C_{10} and cyclo-C_{14} were more thermodynamically, kinetically, dynamically, and optically stable compared with the acknowledged cyclo-C_{18}, and were potential candidates for zero-dimensional carbon rings. Cyclo-C_n (n = 10 and 14) show similar molecular semiconductor characteristics to the acknowledged cyclo-C_{18}. The carbon atoms were sp hybridized in cyclo-C_{10}, cyclo-C_{14}, and cyclo-C_{18}. Cyclo-C_{14} and cyclo-C_{18} had alternating abnormal single and triple bonds, but cyclo-C_{10} had equal bonds. Cyclo-C_{10}, cyclo-C_{14}, and cyclo-C_{18} with large aromaticities had out-of-plane and in-plane π systems, which were perpendicular to each other. The number of π electrons in the out-of-plane and in-plane π systems, respectively, followed the standard Hückel aromaticity rule. Simulated UV-vis-NIR spectra indicated similar electronic structures of cyclo-C_{14} and cyclo-C_{18}.

Introduction

The carbon atom attracts a great deal of attention because it is a fundamental atom in organic compounds and is the constituent atom of many useful materials. For example, there are pure carbon materials, including zero-dimensional fullerene,[1] one-dimensional nanotubes,[2] two-dimensional graphene,[3] and three-dimensional diamond[4] and graphite. They are well-known as allotropes of carbon atoms and are useful in many fields due to their unique electronic structures and physicochemical properties. In the past, fullerene was the only zero-dimensional allotrope of carbon atoms. Very recently, the successful synthesis of cyclo-C_{18} has been ground-breaking in carbon chemistry and means a second type of zero-dimensional allotrope of carbon atoms.[5]

In fact, early experiments on pure carbon clusters date back to 1954, using a heated substrate as the cluster source.[6] After that, there were several experimental and theoretical studies on cyclo-C_n. The synthesis and X-ray crystal structure of a direct precursor of cyclo-C_{18} was described in 1989. The results of time-of-flight mass spectroscopy recognize cyclo-C_{18} as the predominant fragmentation pattern with flash heating experiments on this precursor.[7] In addition, Tobe and Diederich *et al.* synthesized a number of precursors of cyclo-C_{18} with well-defined cyclic geometries and readily removable groups. These precursors eventually generated cyclo-C_{18} by laser desorption induced [4+2] cycloreversion (retro-Diels–Alder reaction), decarbonylation or [2+2] cycloreversion.[8,9] Rubin revealed that cyclo-C_{18} can be highly stabilized as a ligand in a complex, characterized by X-ray crystallography.[10] Furthermore, mass spectral evidence of C_{18} is clearly detected during studies of the fullerene-formation mechanism.[11] For example, the coalescence of cyclo-C_{30} predominantly produces buckminsterfullerene (C_{60}), and the small rings cyclo-C_{18} and cyclo-C_{24} preferentially produce fullerene C_{70} through distinct intermediates.[11] The electronic spectra of C_{18} and C_{22} were detected in the gas phase by a mass-selective resonant two-color two-photon ionization technique coupled to a laser ablation source, and the absorption spectrum of C_{14} was also observed.[12] Another method to generate small carbon cluster ions is presented *via* reaction with HCN.[13] Some of the detected cyanopolyynes were also observed in the

[a] *Institute for Chemical Physics & Department of Chemistry, School of Science, State Key Laboratory of Electrical Insulation and Power Equipment & MOE Key Laboratory for Nonequilibrium Synthesis and Modulation of Condensed Matter, Xi'an Jiaotong University, Xi'an 710049, China. E-mail: xzhao@mail.xjtu.edu.cn*
[b] *Department of Physics, National University of Singapore, Singapore 117551, Republic of Singapore*
[c] *College of Chemical Engineering and Technology, Tianshui Normal University, Tianshui, 741001, China*
[d] *Fukui Institute for Fundamental Chemistry, Kyoto University, Kyoto 606-8103, Japan*
[e] *Institute for Molecular Science, Okazaki, 444-8585, Japan*

† Electronic supplementary information (ESI) available. See DOI: 10.1039/d0cp00167h

interstellar medium. Circumstellar carbon condensation processes in the atmospheres of carbon-rich stars, which are similar to those studied in the laboratory, are suggested as possible synthetic sources.[14–17] Although there are many pieces of evidence for cyclo-C_n clusters, the cyclo-C_{18} geometry was not determined experimentally until 2019.[5]

The previous theoretical investigations contribute much to studying the geometries of cyclo-C_n.[18–21] However, there are lots of controversies regarding the alternating bonds or equal bonds for cyclo-C_n from the viewpoints of experiment and theory. In the case of $N \leq 4$, the bond-length non-alternating cumulenic structure $[D_{(2N+1)h}]$ for monocyclic carbon $4N + 2$ is found to be the most stable, but this structure becomes unstable when $N \geq 5$.[22] Then the bond-length alternating structure $[C_{(2N+1)h}]$ becomes the most stable among the ring-shaped clusters. However, the results of the local-density approximation show that rings C_{4N+2} present no alternation (*i.e.*, aromatic behavior is retained) until very large sizes ($N > 20$).[23] Furthermore, the Monte Carlo method reveals that there are different configurations with an increasing number of carbon atoms, from linear to monocyclic rings and then polycyclic rings to fullerenes.[24] The previous MP2 and LDA calculations on C_{20}, C_{24}, and other clusters indicate that a cage-like fullerene structure may be lowest in energy, followed by cup-like or graphitic "open fullerene" structures and then monocyclic rings.[25–29] Clearly, the theoretical results cannot be confirmed because there is no exact experimental data on rings C_{4N+2} and the two sides still cannot convince each other. Except for the above-mentioned theoretical study on the geometries of cyclo-C_n, there are also several theoretical works focused on the vibrational and electronic spectra to study the electronic structures of cyclo-C_n.[30–32] However, the electronic structures seriously rely on the molecular geometries.

After the successful synthesis and characterization of cyclo-C_{18} with high-resolution atomic microscopy, the alternating bonds of cyclo-C_{18} are clearly revealed.[5] During previous studies on carbon clusters, the other cyclo-C_n were also detected in experiments.[33,34] The synthesis of cyclo-C_{18} encourages both experimental and theoretical researchers to explore the stabilities and physicochemical properties of cyclo-C_n. In the similar case of polyacetylene, previous studies reported that HF (LDA and GGA) tends to overestimate (underestimate) the degree of bond-length alternation in polyacetylene, while hybrid density functional theory (DFT), as well as the Møller–Plesset second-order perturbation theory, reproduces the experimental degree well.[22] Luckily, there is also the cyclo-C_{18} benchmark to select a suitable theoretical method. Herein, we explored the stabilities of cyclo-C_n ($4 \leq n \leq 34$) with hybrid DFT,[35] and cyclo-C_n ($10 \leq n = 4N + 2 \leq 34$, N is an integer) would be the thermodynamically stable molecules. In particular, cyclo-C_n ($n = 10$ and 14) with two similarly perpendicular π systems, including in-plane and conventional out-of-plane π systems, had larger aromaticities and higher stabilities than the acknowledged cyclo-C_{18}. Similar semiconductor characteristics to cyclo-C_{18} were also found for cyclo-C_n ($n = 10$ and 14), which were respected as potential molecular semiconductor devices.

Calculation methods

The optimizations of cyclo-C_{18} were carried out with B3LYP/6-31G(d,p) and M062X/6-311G(d,p) (Fig. S1 in ESI†).[36–38] The results of M062X/6-311G(d,p) are consistent with the experimental results, possessing similar alternating bond lengths (1.35/1.34 Å and 1.23/1.20 Å).[5] In addition, Lu *et al.* reported that the results based on ωB97XD/def2-TZVP are in accordance with the results of CCSD/def-TZVP for cyclo-C_n.[39] Following this report, we carried out ωB97XD/def2-TZVP to optimize cyclo-C_n ($n = 10$, 14, and 18) compared with the results from M062X/6-311G(d,p). As shown in Fig. S2 (ESI†), the results also work well for the optimization of cyclo-C_n ($n = 10$, 14, and 18). Thus, we optimized cyclo-C_n ($4 \leq n \leq 34$) with M062X/6-311G(d,p), and the optimizations of cyclo-C_n ($4 \leq n \leq 34$) were without any imaginary frequency on M062X/6-311G(d,p). The thermodynamically optimal cyclo-C_n ($10 \leq n = 4N + 2 \leq 34$, N is an integer), with lower energies per carbon atom than the adjacent atoms, attract our interest, especially cyclo-C_{10}, cyclo-C_{14}, and cyclo-C_{18}. In order to clarify the electronic structures of cyclo-C_n ($n = 10$, 14, and 18), we carried out natural bond orbital analysis and obtained UV-vis-NIR spectra on the M062X/6-311G(d,p) level.[40,41] The aromaticities of cyclo-C_n ($n = 10$, 14, and 18) were evaluated with nucleus-independent chemical shifts (NICS),[42–44] a simple and efficient aromaticity probe. All of the above calculations were carried out with the Gaussian 16 program package.[45]

In addition, standard *ab initio* molecular dynamics (MD), in which a Verlet algorithm was used to integrate Newton's equations of motion, were simulated on the Perdew–Burke–Ernzerhof (PBE) functional-style generalized gradient approximation (GGA) for the optimal cyclo-C_n ($n = 10$, 14, and 18) under a micro-canonical (*NVE*) ensemble with the VASP program package.[46–49] The thermodynamically stable cyclo-C_n ($n = 10$, 14, and 18) were optimized again with VASP to obtain the initial positions of the molecular dynamic calculations. The default cut-off energy for the pseudopotentials is 400 eV, and the tetragonal lattices are 20 Å for all systems. The three-dimensional periodic boundary condition with a minimum inter-molecular distance of 12 Å was used for all cases to ensure negligible intermolecular interactions. Besides, an automatic *k*-point mesh ($1 \times 1 \times 1$) was generated using a gamma centered grid. The time step is one femtosecond, and the constant temperature considered is 300 K. All of the above-mentioned calculations can be repeated with the corresponding program packages and theoretical methods. Notably, there will be slight deviations of the results with different versions of the software and CPU, but these deviations will not affect the conclusions.

Results and discussion

The higher stabilities of cyclo-C_n ($n = 10$ and 14) compared to acknowledged cyclo-C_{18}

Cyclo-C_n ($4 \leq n \leq 34$) were optimized with different spin multiplicities on the M062X/6-311G(d,p) level to determine their ground states. As shown in Table S1 (ESI†), cyclo-C_n ($13 \leq n \leq 34$) with odd carbon atoms have triplet ground

states, and the other cyclo-C_n ($4 \leq n \leq 34$) have singlet ground states. The singlet cyclo-C_n (n = 5, 7, and 9) were non-planar. Cyclo-C_{11} had a singlet ground state instead of triplet because the relatively small ring had well-delocalized electrons and a close annulene. The spin density maps of triplet cyclo-C_n ($n = 2m + 1$, m = 6–16) are shown in Fig. S3 (ESI†). It is clear that triplet cyclo-C_n ($n = 2m + 1$, m = 6–16) consist of annulene and alkynyl. The spin electrons are almost localized in the annulene part. Cyclo-C_n ($4 \leq n \leq 34$) with triplet ground states were not stable because of their radical characters.[50,51] Therefore, we did not consider these cyclo-C_n ($4 \leq n \leq 34$) with triplet ground states.

The thermodynamic stabilities of cyclo-C_n ($4 \leq n \leq 34$) were explored with the energy per carbon atom in the optimal cyclo-C_n ($4 \leq n \leq 34$) with the ground states. This method has been previously used in exploring the thermodynamic stability of another allotrope of carbon, fullerenes, and was also carried out to clarify the reason why C_{60} and C_{70} possess the largest yield among fullerenes.[52,53] As shown in Fig. 1a, each carbon atom in cyclo-C_n ($10 \leq n = 4N + 2 \leq 34$, N is an integer) possesses a lower energy than those in its adjacent rings, meaning that cyclo-C_n ($10 \leq n = 4N + 2 \leq 34$) were thermodynamically stable molecules. With increasing n, the energies per carbon atom of cyclo-C_n ($4 \leq n \leq 34$) converged to a constant. Cyclo-C_{10} and cyclo-C_{14} have lower energies per carbon atom than their respective adjacent homologues. The gaps between the energies per carbon atom of cyclo-C_{10} and cyclo-C_{14} and their homologues are larger than that of cyclo-C_{18}. Thus, cyclo-C_{10} and cyclo-C_{14} were more thermodynamically stable than cyclo-C_{18}. In addition, these findings suggested that the thermodynamically stable cyclo-C_n ($10 \leq n \leq 34$) followed the $n = 4N + 2$ rule.

Within the validity of Koopmans' theorem, the energy of the highest occupied molecular orbital (HOMO) is the negative ionization potential.[54,55] The lower the energy of the HOMO is, the more difficult ionization is for molecules. As shown in Fig. 1b, when $n = 4N + 2$, cyclo-C_n ($4 \leq n \leq 34$) with singlet ground states possess lower HOMO energies than their adjacent molecules. In particular, cyclo-C_{10} and cyclo-C_{14} have lower HOMO levels than cyclo-C_{18}. In addition, the energies of the lowest unoccupied molecular orbitals (LUMOs) of cyclo-C_{10} and cyclo-C_{14} are higher than that of cyclo-C_{18}. A higher LUMO energy means that it is more difficult to obtain electrons for neutral molecules. Based on the above discussion on HOMOs and LUMOs, cyclo-C_{10} and cyclo-C_{14} were more chemically inert than cyclo-C_{18}.

Meanwhile, the HOMO–LUMO gaps for singlet cyclo-C_n ($4 \leq n \leq 34$) also followed the $4N + 2$ rule. When $n = 4N + 2$ for cyclo-C_n ($4 \leq n \leq 34$), it is clear that the HOMO–LUMO gaps (Fig. 1c) decrease with the increasing number of carbon atoms and eventually converge to a constant. In particular, cyclo-C_{10} and cyclo-C_{14} possess much larger HOMO–LUMO gaps, and Fig. 2 shows their HOMOs and LUMOs. From the viewpoint of optical polarizability, a small HOMO–LUMO gap means small excitation energies to manifold excited states.[56] The much larger HOMO–LUMO gap for cyclo-C_{10} could be explained by the distribution of its HOMO, which is different from the HOMOs of cyclo-C_{14} and cyclo-C_{18}. In fact, the geometry of cyclo-C_{10} was a ring with non-alternating bonds, distinct from the alternating bonds in cyclo-C_{14} and cyclo-C_{18}. A similar result for a cumulenic molecule with a larger HOMO–LUMO gap than acetylenic molecules also occurs for linear C_n clusters.[57,58] In short, cyclo-C_{10} and cyclo-C_{14} were more inert to illumination than cyclo-C_{18}. The HOMO–LUMO gap seriously relies on the theoretical method.[59] Cyclo-C_{18} would be a novel molecular device as a semiconductor.[5] In order to reveal the similar or improved semiconductor characteristics of cyclo-C_{10} and cyclo-C_{14}, the HOMO–LUMO gaps of cyclo-C_n (n = 10, 14, and 18) on M06-2X/6-311G(d,p) were corrected following:

$$C_n^{Corr}(gap) = (C_{60}^{Exp}(gap) \times C_n^{Theo}(gap))/C_{60}^{Theo}(gap),$$

where $C_{60}^{Exp}(gap)$ and $C_{60}^{Theo}(gap)$ are the HOMO–LUMO gap of fullerene C_{60} from experiment (2.30 eV)[60] and on M062X/6-311G(d,p) (4.50 eV); $C_n^{Theo}(gap)$ represents the HOMO–LUMO gaps of cyclo-C_n (n = 10, 14, and 18) on M062X/6-311G(d,p), which are 7.41 eV, 5.75 eV, and 5.33 eV, respectively; $C_n^{Corr}(gap)$ are the corrected HOMO–LUMO gaps of cyclo-C_n (n = 10, 14, and 18). $C_n^{Corr}(gap)$ would be close to the experimental HOMO–LUMO gaps of cyclo-C_n (n = 10, 14, and 18). The reason why we selected the HOMO–LUMO gap of C_{60} as the correction factor is that C_{60} and cyclo-C_n (n = 10, 14, and 18) are allotropes of carbon atoms. $C_n^{Corr}(gap)$ of cyclo-C_n (n = 10, 14, and 18) are 3.78 eV, 2.94 eV, and 2.72 eV, respectively. Clearly, cyclo-C_n

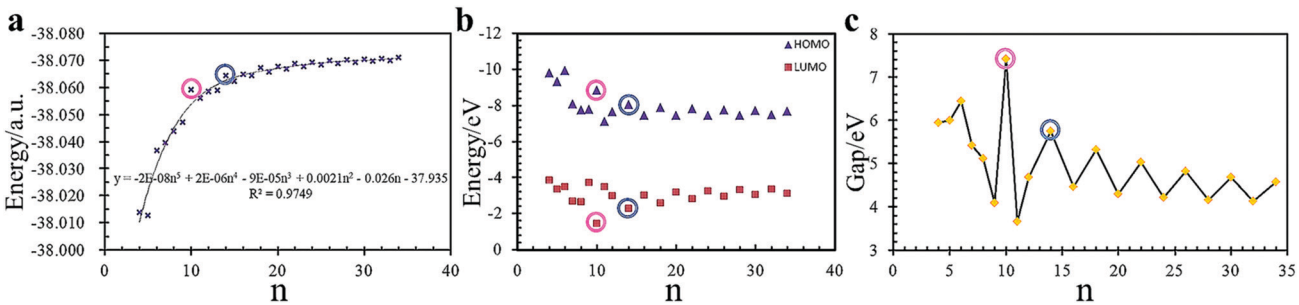

Fig. 1 (a) The energies per carbon atom of cyclo-C_n ($4 \leq n \leq 34$), (b) the HOMO and LUMO energy levels and (c) HOMO–LUMO gaps for cyclo-C_n ($4 \leq n \leq 34$) with singlet ground states based on M062X/6-311G(d,p). Cyclo-C_{10} and cyclo-C_{14} are marked with pink and blue circles, respectively.

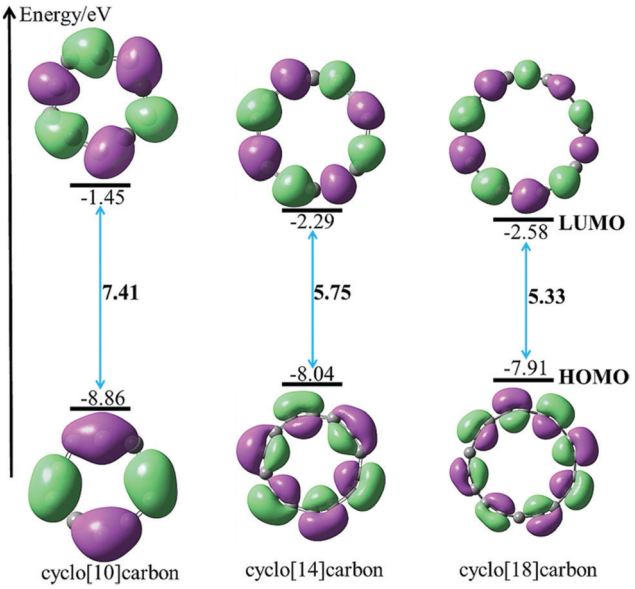

Fig. 2 The distribution of HOMO and LUMO for cyclo-C_n (n = 10, 14 and 18) based on M062X/6-311G(d,p).

(n = 10 and 14) also showed molecular semiconductor characteristics similar to cyclo-C_{18}. Electronic mobility depends on the HOMO–LUMO gaps.[61] Thus, the electronic mobility of cyclo-C_{18} was the highest, followed by cyclo-C_{14} and cyclo-C_{10}.

In order to further compare the stabilities of cyclo-C_n (n = 10, 14, and 18), *ab initio* MD simulations were carried out to explore the dynamic stability. The stabilities of molecules are evaluated *via* the amplitude of changing energies, bond lengths or bond angles with changing time.[62–65] Here, we considered the amplitude of energies on different time scales as a function of stability. As shown in Fig. 3, the dynamic study shows that the energy differences between the maximum and the minimum energy are 0.99, 1.18, and 1.47 eV for cyclo-C_n (n = 10, 14, and 18) after 0.5 ps at 300 K, respectively. Thus, the dynamic stabilities of cyclo-C_n (n = 10 and 14) were superior to that of the acknowledged cyclo-C_{18}. In other words, the geometries of cyclo-C_n (n = 10 and 14) were more difficult to deviate from their optimal geometries than cyclo-C_{18}.

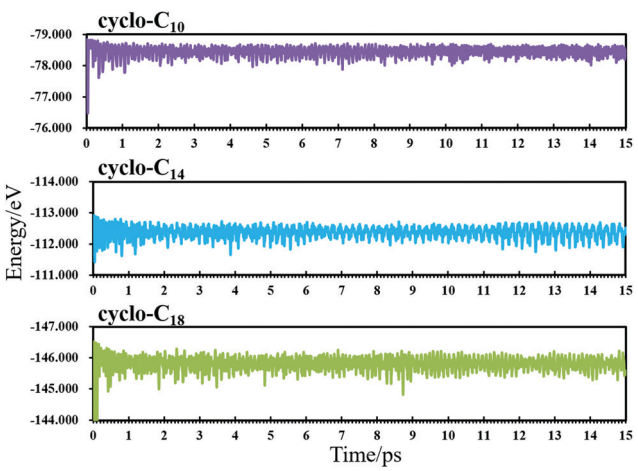

Fig. 3 The energies of cyclo-C_n (n = 10, 14 and 18) at different times.

In order to explore the stability of cyclo-C_n (n = 10, 14, and 18) at different temperatures, *ab initio* MD simulations were also carried out at different temperatures. The energy profiles of MD on cyclo-C_n (n = 10, 14, and 18) are shown in Fig. S4–S6 (ESI†). As shown in Fig. S4–S6 (ESI†), the energies of cyclo-C_n (n = 10, 14, and 18) significantly fluctuate, especially above 1000 K. Furthermore, the maximum energy differences after 0.5 ps for cyclo-C_n (n = 10, 14, and 18) at different temperatures are shown in Fig. 4. There is an approximately linear relation between the maximum energy differences and temperatures after 0.5 ps for cyclo-C_n (n = 10, 14, and 18). As shown in Fig. 4, above 500 K, the maximum energies for cyclo-C_n (n = 10, 14, and 18) are larger than 2 eV, 3 eV, and 4 eV, respectively, indicating a large fluctuation of the geometries of cyclo-C_n (n = 10, 14, and 18). Clearly, the larger the size of cyclo-C_n is, the more unstable it will be at much higher temperature. Considering previous research on the stability of carbon clusters,[24] we thought that cyclo-C_n (n = 10, 14, and 18) would be unstable, or their more stable conformations have fullerene-like geometries above 500 K.

In conclusion, the thermodynamic stabilities of cyclo-C_n ($4 \leq n \leq 34$) followed the $n = 4N + 2$ (N is an integer) rule when $n > 6$. In particular, the thermodynamic stabilities,

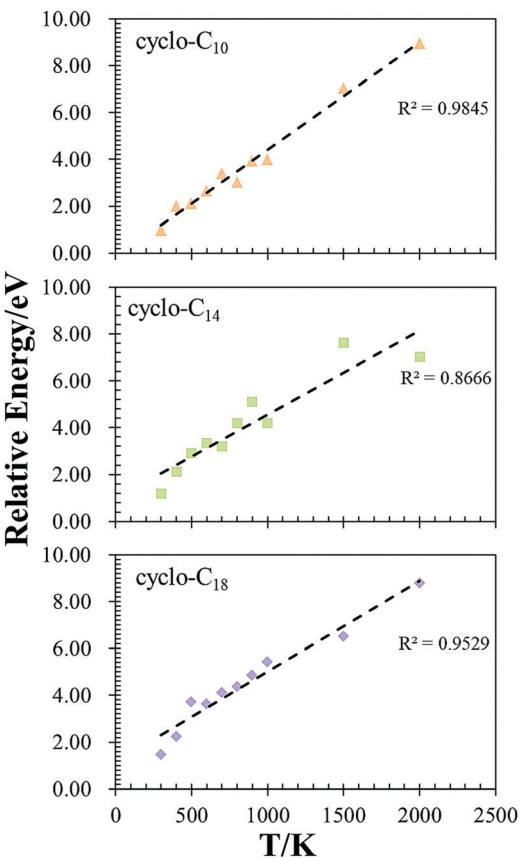

Fig. 4 The energy differences between the largest energy and lowest relative energy for cyclo-C_n (n = 10, 14, and 18) after 0.5 ps at different temperatures.

chemically kinetic stabilities, photostabilities, and dynamic stabilities of cyclo-C_n (n = 10 and 14) were superior to those of the acknowledged cyclo-C_{18}. In addition, the sequence of stabilities for cyclo-C_n (n = 10, 14, and 18) followed cyclo-C_{10} > cyclo-C_{14} > cyclo-C_{18}. Thereby, it was conservative to theoretically predict that it was possible to synthesize and isolate cyclo-C_{10} and cyclo-C_{14} following the synthesis of the first carbon ring cyclo-C_{18}. Furthermore, besides the recent method to prepare cyclo-C_{18}, there are also several methods, including flash heating and laser vaporization, which were carried out to prepare the precursors of cyclo-C_{18}, oxides and metal complexes in the past.[7–9] All of these methods could be good choices for trying to prepare cyclo-C_{10} and cyclo-C_{14}. This prediction was consistent with the previous point that cyclo-C_{14} would be the first carbon ring, with extended Hückel calculations.[18]

The geometries of cyclo-C_n (n = 10, 14, and 18)

The geometries of cyclo-C_n (n = 10, 14, and 18) are shown in Fig. 5, and their geometrical parameters, including bond lengths and bond angles, are listed in Table S2 (ESI†). The maximum distances between two arbitrary atoms are almost constant, 4.14/4.11 Å for cyclo-C_{10}, 5.76 Å for cyclo-C_{14}, and 7.40 Å for cyclo-C_{18}. All of these maximum distances in cyclo-C_n (n = 10, 14, and 18) are close to the diameter of the rings. In general, therefore, this means that the geometries of cyclo-C_n (n = 10, 14, and 18) were close to the standard circle. The circular degree (P) was calculated for cyclo-C_n ($10 \leq n \leq 34$, $n = 2N$). We calculated P for cyclo-C_n ($10 \leq n \leq 34$, $n = 2N$) following the formula:

$$P = \frac{\sum_{1}^{n} (r_i - R_i)}{n}.$$

As shown in Fig. 6, r_i and R_i are the radius of circumcircle and incircle for $\angle 2$, respectively. The r_i is the maximum distance between atom 2 and others. The O_i is the intersection of two adjacent angular bisectors. Then, R_i is the distance between O_i and the bond between atoms 2 and 3. The results of P in Table 1 reveal that with increasing n, the shape of cyclo-C_n ($10 \leq n \leq 34$, $n = 2N$) is much closer to the circle.

The bond lengths in cyclo-C_{10} are equal, and the annulene of cyclo-C_{10} contributed to the larger HOMO–LUMO gap. Alternating bonds, including abnormal single bonds and triple bonds, occurred in cyclo-C_{14} and cyclo-C_{18}. The triple bonds in cyclo-C_{14} and cyclo-C_{18} are 1.25 Å and 1.23 Å, respectively, which are a little longer than the normal C≡C triple bond (1.20 Å). However, the single bonds (1.32 Å and 1.35 Å) in cyclo-C_{14} and cyclo-C_{18} are shorter than normal C-C single bonds (1.50 Å). The abnormal single and triple bonds in cyclo-C_{14} and cyclo-C_{18} indicated a higher contribution of the *s* shell of atomic orbitals. Furthermore, the abnormal double bonds in cyclo-C_{10} and abnormal single and triple bonds in cyclo-C_{14} and cyclo-C_{18} could be confirmed with bond orders.[66] The Mayer bond orders (MBOs) between two adjacent carbon atoms in cyclo-C_{10} are 1.78, smaller than 2. Similarly, the MBOs in cyclo-C_{14}/cyclo-C_{18} are 1.48/1.28 and 2.14/2.45 for the abnormal single and triple bonds, respectively. In cyclo-C_{14} and cyclo-C_{18}, the MBOs for the abnormal single and triple bonds are clearly larger than 1 and smaller than 3, respectively. The alternate bond orders also indicated alternating bonds in cyclo-C_{14} and cyclo-C_{18}.

The distortions of molecules can be defined by the difference between ideal angles based on different hybridizations of carbon atoms and real angles in the target molecules. Carbon atoms in cyclo-C_{10}, cyclo-C_{14}, and cyclo-C_{18} perform as sp hybridized, which was revealed *via* natural bond orbital analysis. The ideal angle is 180° for sp carbon atoms. The angles in cyclo-C_n (n = 10, 14, and 18) are alternative. Thus, we defined the average angles as real angles. The average angles are 144.00°, 154.28°, and 160.00° for cyclo-C_n (n = 10, 14, and 18), respectively. Thus, the distortions of cyclo-C_n (n = 10, 14, and 18) are 36.0°, 25.7°, and 20.0°, respectively. The distortions of cyclo-C_n (14 and 18) are similar. Notably, the distortion of cyclo-C_{10}, performing as an annulene with equal bond lengths, is larger than that of cyclo-C_n (14 and 18).

The electronic structures and aromaticities of cyclo-C_n (n = 10, 14, and 18)

The natural bond orbital (NBO) results showed that the carbon atoms were sp hybridized in cyclo-C_n (n = 10, 14, and 18), thus each carbon atom had two perpendicular p orbitals. In addition, the nucleus-independent chemical shifts (NICS) of cyclo-C_n (n = 10, 14, and 18) are shown in Table 1. Cyclo-C_{14} has the smallest NICS (−32.12) and NICS(1)_ZZ (−74.89), followed by

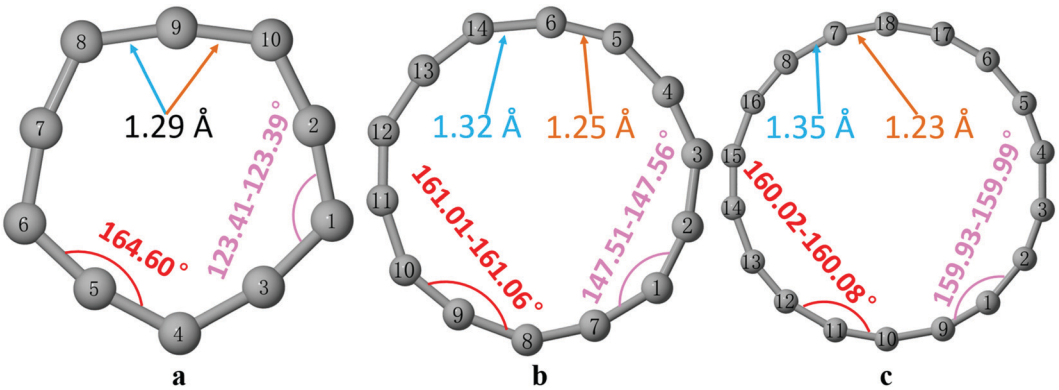

Fig. 5 The geometries of (a) cyclo-C_{10}, (b) cyclo-C_{14}, and (c) cyclo-C_{18} on M062X/6-311G(d,p).

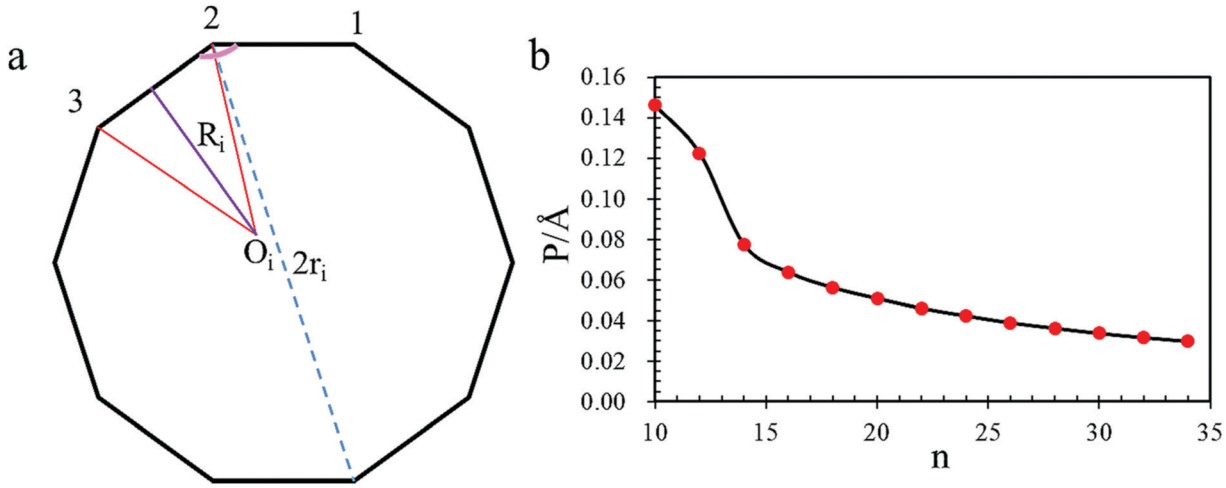

Fig. 6 (a) Schematic of how to calculate the circular degree; (b) the results of circular degrees for cyclo-C_n ($10 \leq n \leq 34$, $n = 2N$).

Table 1 The nucleus-independent chemical shifts for cyclo-C_n (10, 14, and 18)

	NICS[a]	NICS(1)_ZZ[b]
Cyclo-C_{18}	−16.67	−40.98
Cyclo-C_{14}	−32.12	−74.89
Cyclo-C_{10}	−29.45	−57.71

[a] Based on the center of mass for the rings.[32] [b] Based on the π contribution to the out-of-plane *zz* tensor component.[33]

cyclo-C_{10} with NICS (−29.45) and NICS(1)_ZZ (−57.71). Clearly, the aromaticity of cyclo-C_{14} is the largest, and the aromaticity of cyclo-C_{18} is the smallest. It is well known that the aromaticity of a molecule is related to molecular stability.[67,68] Molecules with larger aromaticity have higher stability. The results of aromaticity again confirmed that the stabilities of cyclo-C_{14} and cyclo-C_{10} were higher than that of cyclo-C_{18}.

Based on the analysis of NBO and aromaticities of cyclo-C_n (n = 10, 14, and 18), it can be deduced that there were several delocalized π electrons on cyclo-C_n (n = 10, 14, and 18). Here, we studied the π systems of cyclo-C_n (n = 10, 14, and 18) with molecular orbitals and localized orbital locator (LOL) *via* Multiwfn.[69,70] All of the π orbitals of cyclo-C_n (n = 10, 14, and 18) are shown in Fig. S7–S9 (ESI†). As shown in Fig. S7–S9 (ESI†), the number of π orbitals is equal to the number of carbon atoms in cyclo-C_n (n = 10, 14, and 18). These π orbitals could be divided into two types, including in-plane and out-of-plane π orbitals, because of two perpendicular p orbitals on each carbon atom in cyclo-C_n (n = 10, 14, and 18).

In order to gain further insight into the π electrons, the localized molecular π orbitals of cyclo-C_n (n = 10, 14, and 18) are shown in Fig. 7. The π orbitals, including in-plane and out-of-plane π orbitals, of cyclo-C_n (n = 10, 14, and 18) were similar to each other. The results of π-LOL in Fig. 7 reveal that the π electrons of cyclo-C_n (n = 10, 14, and 18) are delocalized on the whole molecules. Similarly, two perpendicular π systems with $4N + 2$ π electrons, respectively, follow the Hückel aromaticity rules. The number of π electrons can be calculated with the

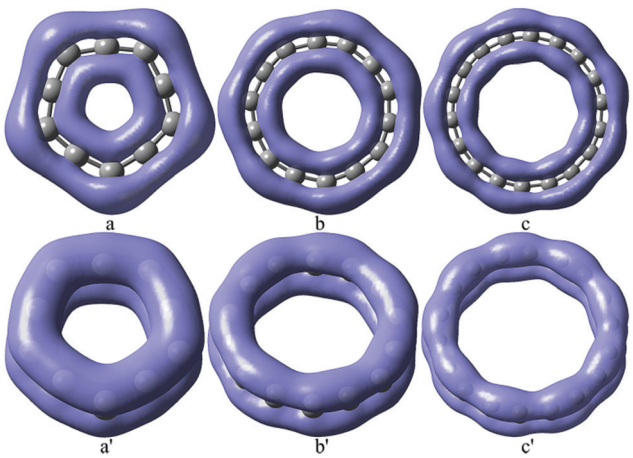

Fig. 7 The localized molecular orbitals for cyclo-C_{10} (a and a′), cyclo-C_{14} (b and b′) and cyclo-C_{18} (c and c′).

number of π molecular orbitals (Fig. S7–S9 (ESI†)) and the number of electrons on sp carbon atoms. For example, cyclo-C_{10} has five in-plane π orbitals and five out-of-plane π orbitals. Thus it has 10 electrons in each delocalized π orbital, and the total number of π electrons is 20. On the other hand, there are 10 sp carbon atoms in cyclo-C_{10}, and the total number of electrons is 60. Each atom has one nonbonding orbital with 20 electrons and one sp σ bond with 20 electrons. There are also 20 π electrons, which are delocalized on two delocalized π orbitals, and each delocalized π orbital in Fig. 7a and a′ has 10 π electrons in cyclo-C_{10}. The number of π electrons on out-of-plane and in-plane delocalized π orbitals, respectively, following the Hückel $4N + 2$ rule, was the reason why cyclo-C_n (n = 10, 14, and 18) had large aromaticity.

The UV-vis-NIR spectra for cyclo-C_n (n = 10, 14, and 18)

UV-vis-NIR spectroscopy is an effective method to clarify the electronic structures of organic molecules in experiment.[71–73] Accordingly, we simulated the UV-vis-NIR spectra of cyclo-C_n (n = 10, 14, and 18) on the M062X/6-311G(d,p) level. As shown in

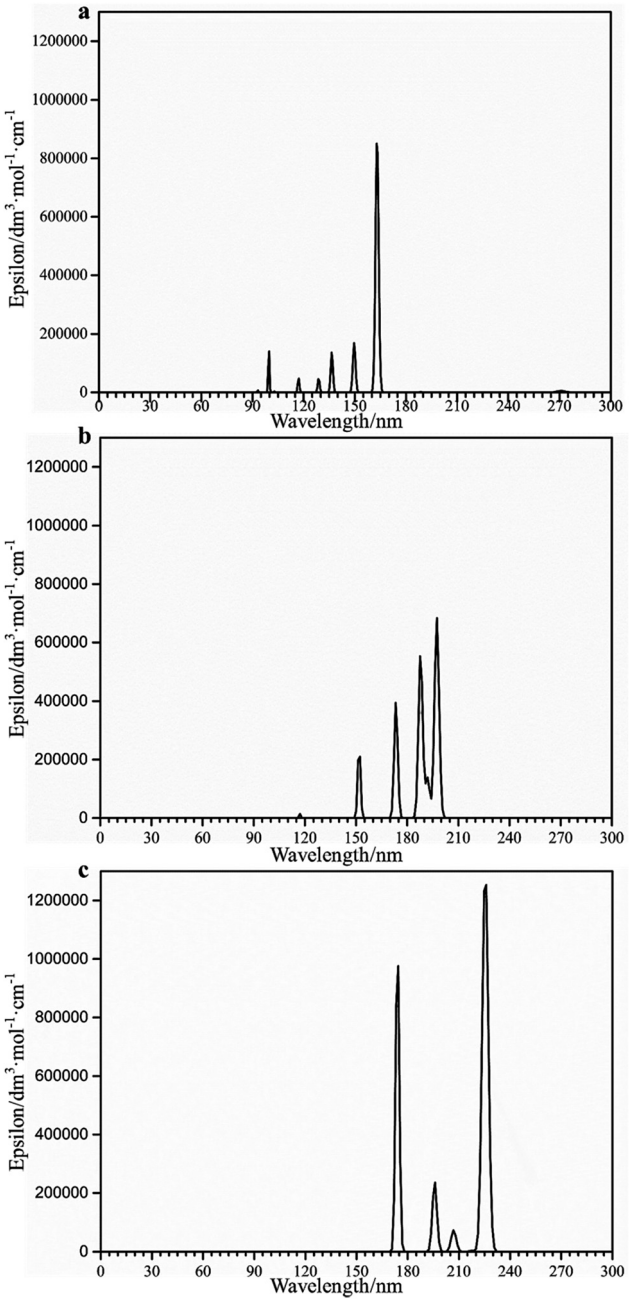

Fig. 8 The simulated UV-vis-NIR absorption spectra for cyclo-C_n (n = 10, 14, and 18) on the M062X/6-311G(d,p) level.

Fig. 8, four main absorption peaks can be observed for cyclo-C_n (n = 10, 14, and 18). Additionally, there are two small absorption peaks in cyclo-C_{10}, distinguished from cyclo-C_n (n = 14, and 18) with alternating bonds. The absorption peaks of cyclo-C_n (n = 10, 14, and 18) in Fig. 8 were from the π–π* transition. The similar absorption peaks for cyclo-C_n (n = 14, and 18) represented similar geometries and electronic structures. With increasing ring size, blue shifts of the four main absorption peaks in cyclo-C_n (n = 10, 14, and 18) occur due to the more delocalized π electrons. The simulated UV-vis-NIR spectra of cyclo-C_n (n = 10, 14, and 18) could assist in further exploration of cyclo-C_n (n = 10, 14, and 18) by experiment.

Conclusions

Herein, the thermodynamic stabilities of cyclo-C_n ($4 \leq n \leq 34$) were explored with density functional theory, and the results revealed that cyclo-C_n ($10 \leq n \leq 34$, $n = 4N + 2$) would be thermodynamically stable, following the Hückel $4N + 2$ rule. Compared with the acknowledged cyclo-C_{18}, cyclo-C_{10} and cyclo-C_{14} possessed higher thermodynamic, kinetic, optical, and dynamic stabilities under 500 K. Accordingly we predicted that cyclo-C_{10} and cyclo-C_{14} could be prepared in future experiments. There were equal double bonds in cyclo-C_{10}, in contrast to the alternating abnormal single bonds and triple bonds in cyclo-C_{14} and cyclo-C_{18}. These geometrical characteristics were also in accordance with the results of Mayer bond orders between two adjacent carbon atoms. Cyclo-C_{18}, cyclo-C_{10}, and cyclo-C_{14} had large aromaticities because they had two perpendicular delocalized π orbitals, including out-of-plane and in-plane π orbitals. The number of π electrons on the out-of-plane and in-plane π orbitals followed the Hückel $4N + 2$ rule. Furthermore, the much larger aromaticities of cyclo-C_{10} and cyclo-C_{14} were also in favor of the higher stabilities of cyclo-C_{10} and cyclo-C_{14} than cyclo-C_{18}. In addition, cyclo-C_{10} and cyclo-C_{14} also showed similar semiconductor characteristics to cyclo-C_{18}, and all would be respected as a new generation of molecular semiconductor devices. The UV-vis-NIR spectra of cyclo-C_n (n = 10, 14, and 18) were simulated as a reference for further experimental study. There have been lots of efforts to prepare cyclo-C_{18}, and all of these methods could be carried out to try to prepare cyclo-C_n (n = 10 and 14) with larger stability than cyclo-C_{18}. Undoubtedly, the successful synthesis and characterization of cyclo-C_{18} has encouraged many researchers to study cyclo-C_n homologues, and based on the present theoretical investigation, we believe that cyclo-C_n (n = 10 and 14) will be potential candidates for zero-dimensional allotropes of carbon atoms and molecular semiconductor devices, as well as cyclo-C_{18}.

Conflicts of interest

There are no conflicts to declare.

Acknowledgements

The National Natural Science Foundation of China (21773181, 21573172) has financially supported this work. X. Z. would like to acknowledge the financial support from the Nanotechnology Platform Program (Molecule and Material Synthesis) of the Ministry of Education, Culture, Sports, Science, and Technology of Japan. Z. Gao is supported by a MOE tier 1 grant R-144-000-402-114.

Notes and references

1 H. W. Kroto, J. R. Heath, S. C. O'Brien, R. F. Curl and R. E. Smalley, *Nature*, 1985, **318**, 162–163.
2 S. Iijima, *Nature*, 1991, **354**, 56–58.

3 K. S. Novoselov, A. K. Geim, S. V. Morozov, D. Jiang, Y. Zhang, S. V. Dubonos, I. V. Grigorieva and A. A. Firsov, *Science*, 2004, **306**, 666–669.
4 J. Robertson, *Mater. Sci. Eng., R*, 2002, **37**, 129–281.
5 K. Kaiser, L. M. Scriven, F. Schulz, P. Gawel, L. Gross and H. L. Anderson, *Science*, 2019, **365**, 1299–1301.
6 R. E. Honig, *J. Chem. Phys.*, 1954, **22**, 126–131.
7 F. Diederich, Y. Rubin, C. B. Knobler, R. L. Whetten, K. E. Schriver, K. N. Houk and Y. Li, *Science*, 1989, **245**, 1088–1090.
8 E. A. Rohlfing, D. M. Cox and A. Kaldor, *J. Chem. Phys.*, 1984, **81**, 3322–3330.
9 Y. Tobe, H. Matsumoto, K. Naemura, Y. Achiba and T. Wakabayashi, *Angew. Chem., Int. Ed. Engl.*, 1996, **35**, 1800–1802.
10 Y. Rubin, C. B. Knobler and F. Diederich, *J. Am. Chem. Soc.*, 1990, **112**, 4966–4968.
11 G. V. Helden, N. G. Gotts and M. T. Bowers, *Nature*, 1993, **363**, 60–63.
12 A. E. Boguslavskiy, H. Ding and J. P. Maier, *J. Chem. Phys.*, 2005, **123**, 034305.
13 M. B. Bell, P. A. Feldman, S. Kwok and H. E. Matthews, *Nature*, 1982, **295**, 389–391.
14 D. C. Parent and S. W. McElvany, *J. Am. Chem. Soc.*, 1989, **111**, 2393–2401.
15 H. W. Kroto, *Int. Rev. Phys. Chem.*, 1981, **1**, 309–376.
16 W. L. Brown, R. R. Freeman, K. Raghavachari and M. Schlüter, *Science*, 1987, **235**, 860–865.
17 J. R. Heath, Q. Zhang, S. C. O'Brien, R. F. Curl, H. W. Kroto and R. E. Smalley, *J. Am. Chem. Soc.*, 1987, **109**, 359–363.
18 R. Hoffmann, *Tetrahedron*, 1966, **22**, 521–538.
19 K. Raghavachari and J. S. Binkley, *J. Chem. Phys.*, 1987, **87**, 2191–2197.
20 V. Parasuk, J. Almlöf and M. W. Feyereisen, *J. Am. Chem. Soc.*, 1991, **113**, 1049–1050.
21 T. Torelli and L. Mitas, *Phys. Rev. Lett.*, 2000, **85**, 1702–1705.
22 M. Saito and Y. Okamoto, *Phys. Rev. B: Condens. Matter Mater. Phys.*, 1999, **60**, 8939–8942.
23 E. J. Bylaska, J. H. Weare and R. Kawai, *Phys. Rev. B: Condens. Matter Mater. Phys.*, 1998, **58**, 7488–7491.
24 G. V. Helden, M. T. Hsu, N. Gotts and M. T. Bowers, *J. Phys. Chem.*, 1993, **97**, 8182–8192.
25 V. Parasuk and J. Almlöf, *Chem. Phys. Lett.*, 1991, **184**, 187–190.
26 M. Feyereisen, M. Gutowski, J. Simons and J. Almlöf, *J. Chem. Phys.*, 1992, **96**, 2926–2932.
27 C. J. Brabec, E. B. Anderson, B. N. Davidson, S. A. Kajihara, Q. M. Zhang and J. Bernholc, *Phys. Rev. B: Condens. Matter Mater. Phys.*, 1992, **46**, 7326–7328.
28 F. Jensen and H. Toftlund, *Chem. Phys. Lett.*, 1993, **201**, 89–96.
29 G. V. Helden, M. T. Hsu, N. G. Gotts, P. R. Kemper and M. T. Bowers, *Chem. Phys. Lett.*, 1993, **204**, 15–22.
30 J. D. Presilla-Márquez, J. A. Sheehy, J. D. Mills, P. G. Carrick and C. W. Larson, *Chem. Phys. Lett.*, 1997, **274**, 439–444.
31 J. D. Presilla-Márquez, J. Harper, J. A. Sheehy, P. G. Carrick and C. W. Larson, *Chem. Phys. Lett.*, 1999, **300**, 719–726.
32 M. Grutter, M. Wyss, E. Riaplov, J. P. Maier, S. D. Peyerimhoff and M. Hanrath, *J. Chem. Phys.*, 1999, **111**, 7397–7401.
33 H. Y. So and C. L. Wilkins, *J. Phys. Chem.*, 1989, **93**, 1184–1187.
34 S. Iijima, *J. Phys. Chem.*, 1987, **91**, 3466–3467.
35 R. G. Parr and W. Yang, *Density Functional Theory of Atoms and Molecules*, Oxford, New York, 1989.
36 A. D. Becke, *J. Chem. Phys.*, 1993, **98**, 5648–5652.
37 Y. Zhao and D. G. Truhlar, *Theor. Chem. Acc.*, 2008, **120**, 215–241.
38 R. Krishnan, J. S. Binkley, R. Seeger and J. A. Pople, *J. Chem. Phys.*, 1980, **72**, 650–654.
39 T. Lu, Q. X. Chen and Z. Y. Liu, 2019, ChemRxiv, DOI: 10.26434/chemrxiv.11320130.v1.
40 A. E. Reed, L. A. Curtiss and F. Weinhold, *Chem. Rev.*, 1988, **88**, 899–926.
41 M. Schnaiter, H. Horvath, O. Möhler, K. H. Naumann, H. Saathoff and O. W. Schöck, *J. Aerosol Sci.*, 2003, **34**, 1421–1444.
42 P. V. R. Schleyer, C. Maerker, A. Dransfeld, H. J. Jiao and N. J. R. V. E. Hommes, *J. Am. Chem. Soc.*, 1996, **118**, 6317–6318.
43 H. Fallah-Bagher-Shaidaei, C. S. Wannere, C. Corminboeuf, R. Puchta and P. V. R. Schleyer, *Org. Lett.*, 2006, **8**, 863–866.
44 Z. F. Chen, C. S. Wannere, C. Corminboeuf, R. Puchta and P. V. R. Schleyer, *Chem. Rev.*, 2005, **105**, 3842–3888.
45 M. J. Frisch, *et al.*, *Gaussian 16, Revision A.03*, Gaussian, Inc., Wallingford CT, 2016.
46 G. Kresse and J. Furthmüller, *Comput. Mater. Sci.*, 1996, **6**, 15–50.
47 G. Kresse, J. Furthmüller and J. Hafner, *Phys. Rev. B: Condens. Matter Mater. Phys.*, 1994, **50**, 13181–13185.
48 G. Kresse and J. Furthmüller, *Phys. Rev. B: Condens. Matter Mater. Phys.*, 1996, **54**, 11169–11186.
49 J. P. Perdew, K. Burke and M. Ernzerhof, *Phys. Rev. Lett.*, 1998, **80**, 891.
50 W. Brand-Williams, M. E. Cuvelier and C. Berset, *LWT-Food Sci. Technol.*, 1995, **28**, 25–30.
51 K. Matyjaszewski and J. H. Xia, *Chem. Rev.*, 2001, **101**, 2921–2990.
52 R. F. Curl, M. K. Lee and G. E. Scuseria, *J. Phys. Chem. A*, 2008, **112**, 11951–11955.
53 R. L. Murry, D. L. Strout and G. E. Scuseria, *Int. J. Mass Spectrom. Ion Processes*, 1994, **138**, 113–131.
54 J. Luo, Z. Q. Xue, W. M. Liu, J. L. Wu and Z. Q. Yang, *J. Phys. Chem. A*, 2006, **110**, 12005–12009.
55 R. Manne and T. Åberg, *Chem. Phys. Lett.*, 1970, **7**, 282–284.
56 R. G. Pearson, *Proc. Natl. Acad. Sci. U. S. A.*, 1986, **83**, 8440–8441.
57 S. J. Yang and M. Kertesz, *J. Phys. Chem. A*, 2008, **112**, 146–151.
58 A. Imamura and Y. Aoki, *Int. J. Quantum Chem.*, 2013, **113**, 423–427.
59 F. Flores, J. Ortega and H. Vázquez, *Phys. Chem. Chem. Phys.*, 2009, **11**, 8658–8675.
60 R. W. Lof, M. A. Van Veenendaal, B. Koopmans, H. T. Jonkman and G. A. Sawatzky, *Phys. Rev. Lett.*, 1992, **68**, 3924–3927.
61 Z. B. Gao, G. Liu and J. Ren, *ACS Appl. Mater. Interfaces*, 2018, **10**, 40702–40709.

62 A. A. Popov, C. B. Chen, S. F. Yang, F. Lipps and L. Dunsch, *ACS Nano*, 2010, **4**, 4857–4871.
63 Z. B. Gao, X. Dong, N. B. Li and J. Ren, *Nano Lett.*, 2017, **17**, 772–777.
64 Z. B. Gao, F. Tao and J. Ren, *Nanoscale*, 2018, **10**, 12997–13003.
65 Y. X. Zhao, M. Y. Li, Y. M. Xiong, S. Rahmani, K. Yuan, R. S. Zhao, M. Ehara, S. Nagase and X. Zhao, *J. Comput. Chem.*, 2019, **40**, 2730–2738.
66 I. Mayer, *Int. J. Quantum Chem.*, 1986, **29**, 477–483.
67 T. M. Krygowski and M. K. Cyrański, *Chem. Rev.*, 2001, **101**, 1385–1419.
68 P. K. Chattaraj and S. Giri, *J. Phys. Chem. A*, 2007, **111**, 11116–11121.
69 T. Lu and F. W. Chen, *J. Comput. Chem.*, 2012, **33**, 580–592.
70 H. Jacobsen, *Can. J. Chem.*, 2008, **86**, 695–702.
71 A. G. Ryabenko, T. V. Dorofeeva and G. I. Zvereva, *Carbon*, 2004, **42**, 1523–1535.
72 A. G. Martynov, J. Mack, A. K. May, T. Nyokong, Y. G. Gorbunova and A. Y. Tsivadze, *ACS Omega*, 2019, **4**, 7265–7284.
73 Y. Zhang, J. A. Alarco, A. S. Best, G. A. Snook, P. C. Talbot and J. Y. Nerkar, *RSC Adv.*, 2019, **9**, 1134–1146.